

# SHORT TERM PREDICTION OF E $\geq$ 10 MeV PROTON FLUXES FROM SOLAR FLARES

George A. Kuck, Capt, USAF

## AIR FORCE WEAPONS LABORATORY

One problem facing the Aerospace Environmental Support Center (Det 1, 4th WW, AWS) is the prediction of ionospheric effects related to energetic proton emissions from the sun. The intensity and duration of these charged particle emissions are related to the optical, radio, and X-ray emissions from the solar flares. Radio and X-ray data give an important indication of proton production. Cm radio bursts with a high flux density and a slope reflecting greater flux values at higher frequencies are often proton productive. Examination of the data summaries has shown that the meter classification of flares as type II or type IV, even though qualitative, should be used in conjunction with the cm radio criteria. The peak intensity of the proton flux  $E \geq 10$  meV correlates better with the integrated 1 to 8 Å X-ray bursts than with the integrated cm radio bursts, peak cm radio flux, or peak X-ray flux. Free-free transition theory was used to relate the X-ray flux. Free-free transition theory was used to relate the X-ray intensities recorded by different satellites with the peak proton fluxes observed at the earth.

Both the anisotropic and isotropic diffusion theories could be used to extrapolate proton fluxes for  $E \geq 10$  meV for over 50% of the particle events. The isotropic diffusion theory uses a diffusion coefficient.

$$D = Mr^\beta$$

It was found that M and  $\beta$  tended to be functions of flare position on the solar disk.

A measurement of the interplanetary flux in near earth space gives a good indication of the polar cap fluxes. It was found that the 30 MHz absorption over the poles during a PCA is proportional to the square root of the integral proton flux  $E \geq 11$  meV in interplanetary space.

$$J = KA^2$$

with  $K = 8 \pm 2$  and J in protons/cm<sup>2</sup>-sec-ster.

Without the moral support of the personnel assigned to the Solar Forecast Center and the Solar Forecast Facility, this report could not have been written. My thanks go to Mr. Ray Cormier of Air Force Cambridge Research Laboratories for allowing me to use his riometer data. The Vela X-ray data were kindly supplied by Dr. Kunz, Dr. Conner, and Dr. Bame of Los Alamos Scientific Laboratories. The author is solely responsible for the opinions and material presented in this report. The consent of the above-mentioned scientists to use their data does not necessarily imply their agreement with the results.

### I. Introduction

One problem facing the Air Weather Service Solar Forecast Center is the prediction of ionospheric effects related to energetic proton emissions from the sun. The intensity, and duration of these charged particle emissions are related to the optical, radio, and X-ray emissions from the solar flares. Data summaries

appearing in pre-published form, such as the Explorer 34 proton results in the Solar-Geophysical Data bulletins published by ESSA (ref. 1) and the Geophysics and Space Data Bulletin by AFCRL (ref. 2), have allowed the evaluation of many important parameters.

The work reported in the paper was done for an operational unit. Therefore,

the data base available to the operational solar forecaster was used. This was not the most precise data base available. Several simplifying assumptions had to be made which will become apparent in this paper. Nevertheless, the results clearly indicate that short-term proton event predictions are possible and indicate certain limitations on several current theories.

An interdisciplinary approach to PCA prediction and ionospheric forecasting allows some effects to be calculated from first principles shortly after the optical flare occurs. Solar radio and X-ray burst observations are useful in determining if protons were actually produced during the flare. These bursts also give an indication of the number of protons produced. The position of the flare on the solar disk and the solar wind velocity can be used to indicate the risetime and the peak intensity of the event in the near earth space. Using the first few proton data points, the proton intensities can be extrapolated into the future. Ground-based magnetic measurements can then be used to indicate the spatial extent of the precipitation and its uniformity. Satellite data and real time magnetic measurements can be used to update the forecasts during the event. On the basis of the extrapolated fluxes, the next step is to calculate the ionization caused by the protons using an atmospheric model and a two-ion D-region model for PCA events to obtain the electron profiles. Finally, the absorption on vertical and oblique paths can be calculated for high-frequency communication systems across the polar regions. Real time satellite and riometer measurements can be used to verify the prediction.

This paper covers several of the different phases of PCA prediction. First, the X-ray characteristics of proton producing flares are examined. Then the two theories relating to particle propagation in the interplanetary medium are investigated for their applicability. Finally, the relationships between 30 MHz riometer absorption and the exospheric proton flux are discussed. The problem of electron profiles and oblique absorption will not be covered in this report. The radio characteristics of the flare and the spatial extent of the polar cap absorption event will not be covered because they have been discussed previously (ref. 3).

## II. General Discussion

In order to meaningfully predict proton fluxes at the earth before the arrival of large numbers of protons, one must use the electromagnetic characteristics of the parent flare. The simplest set of assumptions one can make about the peak proton fluxes are that (1) the peak flux is proportional to the number of particles accelerated by the parent flare,  $N$ , and (2) the transport of the particles to the earth is influenced by the interplanetary medium,  $P$ . Thus, the flux,  $J$  is just

This paper presents some experimental determinations of  $N$  and  $P$ . The actual prediction of proton production has been previously published (ref. 3).

## III. Proton Acceleration and X-Radiation Flux

There are several methods of determining  $N$ , such as integrated or peak radio intensity, H- $\alpha$  flare classification, and integrated or peak X-ray intensity. Of these, the integrated X-ray intensity seems to be the best quantitative measure of proton acceleration. If the number of electrons accelerated during the flare is proportional to the number of protons accelerated, and if the intensity of X rays in some wavelength band is proportional to the number of electrons being accelerated, then the integrated intensity of X-radiation in that band ought to be proportional to the number of protons accelerated. For simplicity, it was assumed that the X-ray bursts had exponential rise and exponential decay time. Then

$$I_{\text{int}} = \int_{-\infty}^0 I_{\text{max}} \exp(t/t_r) dt + \int_0^{\infty} I_{\text{max}} \exp(-t/t_d) dt \quad (2)$$

$$I_{\text{int}} = I_{\text{max}} (t_r + t_d) \quad (3)$$

where  $t_r$  and  $t_d$  are the exponential rise and decay times,  $I_{\text{max}}$  is the maximum X-ray intensity, and  $I_{\text{int}}$  is the integrated X-ray intensity. The use of such a simple relationship allows a forecaster to make predictions with minimum information.

The largest, most consistent X-ray data base available is the Vela X-ray data (refs. 5, 6). The 0.5 to 5 Å X-ray data were integrated using equation (3). The result of plotting the integrated X-ray intensity versus the peak 10-meV proton fluxes observed by IMP F (Explorer 33) is given in figure 1 (ref. 1). Even though these points are not corrected for propagation through the interplanetary space, the correlation is striking.

One must generalize these results shown in figure 1, to those obtainable from different sensors. This was a problem since the integrated X-ray flux presented in figure 1 was a measure of the flux deposited inside the detector after transmission through detector windows. The most commonly used assumption when determining the flux incident on an X-ray detector is that the photon spectrum is a blackbody Planckian spectrum of the form

$$W(\lambda, T) d\lambda \propto \frac{8\pi hc}{\lambda^5} \frac{d\lambda}{e^{hc/\lambda kT} - 1}$$

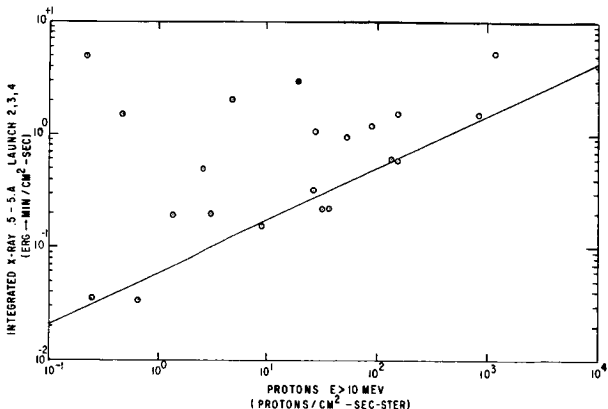


Figure 1. Integrated X-ray flux deposited in 0.5 to 5.0 Å Vela launch 2, 3, 4 detectors vs. peak proton flux ( $E > 10$  meV protons/cm<sup>2</sup>-sec-ster). Propagation factors have not been removed.

In order to compare the data obtained from different satellites, this spectral form was folded into the different detector responses as a function of solar flare temperature. When this form was used, different detectors did not give consistent results. Figure 2 shows the flare

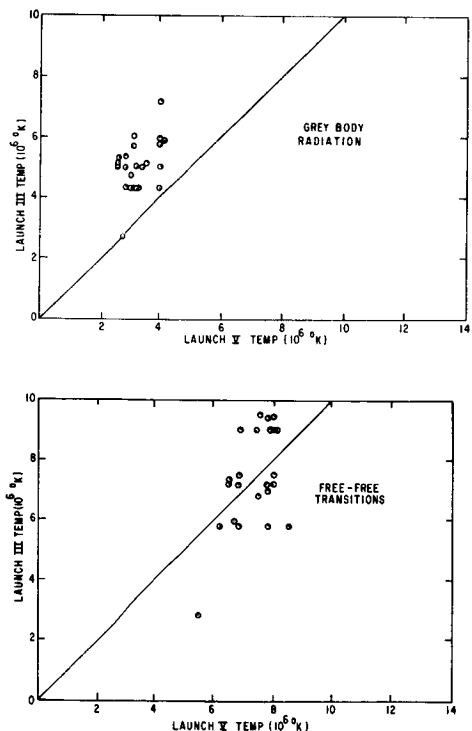


Figure 2. Solar flare temperature Vela launch 2, 3, 4 vs. solar flare temperature Vela launch 5. Figure 2a is the grey body assumption while figure 2b is the free-free transition assumption.

temperatures determined by two different methods from two distinctly different sets of satellite instrumentation. Note that the grey body assumption (fig. 2a) does not fit the data accurately. Furthermore, when the grey body assumption was employed the correlation between the 1 to 8 Å integrated X-ray flux and the peak proton flux disappeared.

The functional form of the X-ray energy spectrum which allowed the correlation between the 1 to 8 Å X-ray flux and the peak proton flux to remain and which better correlated the solar flare temperatures given in figure 2b was

$$W(\lambda, T) d\lambda \propto \frac{d\lambda}{\lambda^2 e^{-hc/\lambda kT}}$$

This is the functional form obtained by assuming the X rays are produced by a Maxwellian distribution of electrons undergoing free-free transitions (i.e., bremsstrahlung) (ref. 7, 8). This assumption allowed the peak proton flux to be correlated with the 1 to 8 Å X-ray flux, which is given in figure 3. Not enough data have been published at the present time to

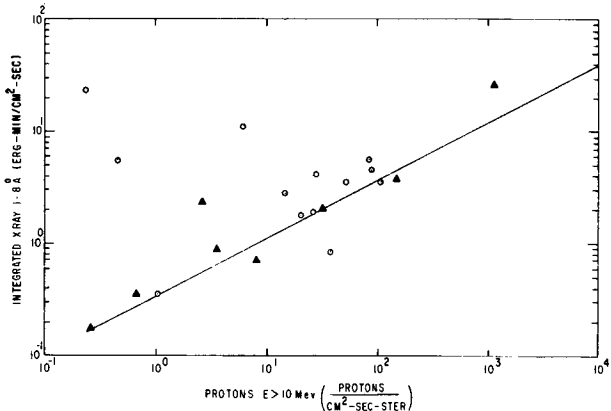


Figure 3. Integrated X-ray flux incident on a detector in the 1 to 8 Å band vs. proton flux  $E > 10$  meV. Points were derived from figure 1 using the free-free transition assumption. Triangle points were derived assuming the average proton flare temperature of  $7 \times 10^6$  °K.

allow the complete verification of this analysis. However, the few points which have been obtained from Explorer 44 are presented in figure 1, but the scatter is well within that expected. The average solar flare temperature for the proton producing flares was  $7 \times 10^6$  °K. This temperature was obtained from the Vela launch 2, 3, 4 sensors using free-free transition theory.

#### IV. Arrival of Protons

There are two theoretical frameworks within which the proton observations could be analyzed. The first is the anisotropic diffusion with boundary theoretical framework (ADB) of Burlaga (ref. 9), while the second is the isotropic diffusion theoretical framework (refs. 10, 11). Both theories have definite shortcomings. These shortcomings are illustrated in figure 4. If the theoretical models were adequate at 10 meV, one would expect systematic trends when plotting the proton risetimes against the  $1/e$  decay times. The scatter in this diagram illustrates the problems involved in attempting to fit the experimental data. Similar plots for  $E > 30$  and  $E > 60$  meV protons do show more systematic results.

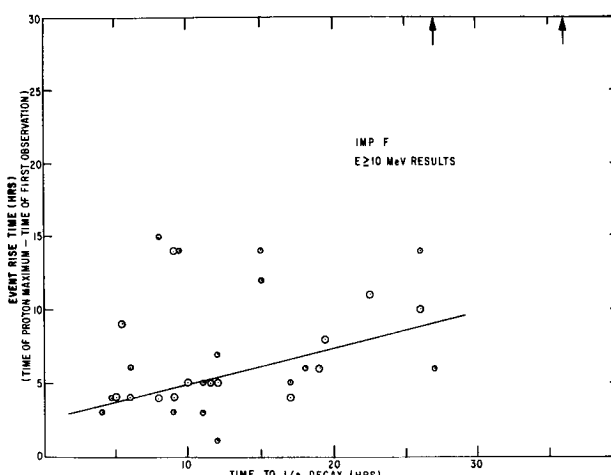


Figure 4. The time in hours it took 10-meV protons to peak as a function of the time it took for the protons to reach  $1/e$  of their maximum value.

The anisotropic diffusion with boundary (ADB) theory assumes that the interplanetary magnetic field lines between the sun and the earth are spirals with irregularities which can effectively scatter the solar protons. The solar proton flux in this theory will be greatest in the direction of the field. Beyond 1 A.U., the scattering centers change so that protons cannot be scattered back into the diffusing region once they have reached the transition region. Thus, in this model, it is assumed that there is an absorbing boundary at some heliocentric distance greater than 1 A.U. Since systematic trends did not appear in applying this theory, and since this theory has been discussed in detail (ref. 3), it will not be examined in any more detail in this paper.

One can also analyze each proton event in terms of the isotropic diffusion theory (refs. 10, 11). In this theory, the diffusion coefficient,  $D$ , is given by

$$D = Mr^\beta \quad (4)$$

where  $r$  is the heliocentric radial distance in A.U., and  $M$  and  $\beta$  are parameters which may and often do depend upon the particle energy  $E$ . The units of  $Mr^\beta$  are  $(\text{hours})^{-2}$ . Krimigis shows that for  $E < 50$  meV, the parameter  $M$  does depend upon the proton energy. Thus, if one wants the time behavior for 10 meV protons, one must use a data base of 10 meV.

It can be shown that

$$t_{\max} = \frac{1}{3M} \frac{r^{2-\beta}}{(2-\beta)} \quad (5)$$

where  $M$  and  $\beta$  are the coefficients given in equation (2) and  $t_{\max}$  is the time it takes for the protons to reach maximum intensity. Since  $t_{\max}$  does depend upon the solar flare heliographic longitude, it is possible to empirically determine  $M$  and  $\beta$  as a function of solar flare position even though such an assumption violates the basic theoretical considerations.

Approximately 80% of the observed events could be analyzed within the isotropic diffusion framework. Figure 5 shows one of these events. This figure also shows that there is an area of agreement between the ADB theory and the isotropic diffusion theory. A certain amount of judgment was necessary in determining  $\beta$  from the graphs of  $1/t$  vs.  $\ln(1/t)^{(3/2-\beta)}$  because of poor time resolution and uncertainties in count rates and particle backgrounds. This event also illustrates what happens when a proton event has considerable structure. Many events showed the characteristic hook at small values of  $1/t$ . The value of  $\beta$  used was that value which best fit the first several values of  $1/t$  and which also adequately fit the long time behavior at small values of  $1/t$ .

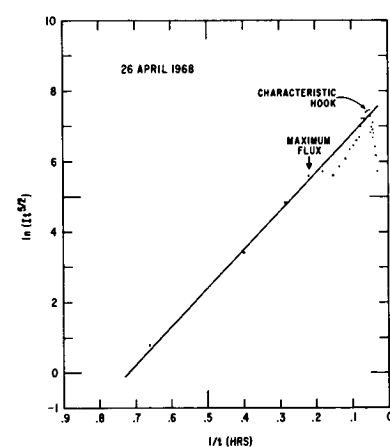


Figure 5. Intensity-time profile during 26 April 1968 event for protons  $E > 10$  meV measured by Explorer 34. This event had considerable structure.

Figure 6 gives scatter plots of  $\beta$  and  $M$  as a function of  $\theta$  for 10 and 30 meV protons as a function of flare position. The  $\theta$  was determined in the ADB theoretical framework (ref. 9). Several features do stand out. The low values of  $\beta$  and  $M$  for  $\theta$  less than 0.25 radian are probably due to the diffusion being one or two dimensional instead of three dimensional as assumed in this analysis. There does seem to be a trend as a function of  $\theta$  for  $\theta > 0.5$  radian. Although there is a large amount of scatter, the higher energy particles tend to have larger values of  $M$  and  $\beta$  than the lower energy particles.

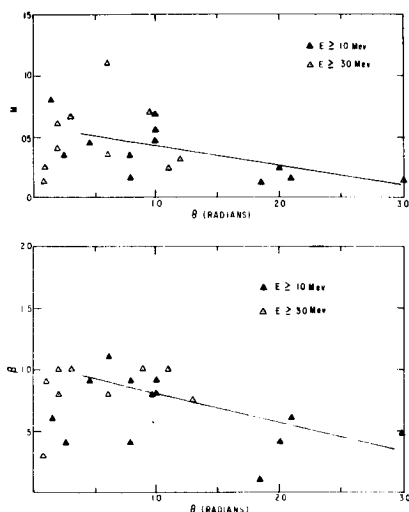


Figure 6. The diffusion coefficients,  $M$  and  $\beta$  as a function of flare position and the Earth-Sun Archimedes spiral angle  $\theta$ . The higher energy particles tend to have higher values of  $M$  and  $\beta$ .

These results can be refined. Better time resolution will lead to less scatter in the data. The better the time resolution, the easier it was to determine  $M$  and  $\beta$ . Data for larger values of  $\theta$  have not yet become available with the necessary count rate accuracy or time resolution.

##### V. RIOMETER ABSORPTION

Once one has predicted the intensity of protons in interplanetary space, one can predict an upper limit to the vertical 30 MHz riometer absorption.

On the basis of theoretical calculations (ref. 12), it can be concluded that the 30 MHz riometer absorption is proportional to the square root of the incident integral particle flux for  $E \geq 11$  meV (ref.

13). An analysis of the Explorer 34 and Thule riometer data has helped confirm this result.

$$J = KA^2$$

where  $J$  is the flux in protons/cm -sec-ster, and  $A$  is the absorption in db of the 30 MHz riometer.

The Explorer 34 data and Thule riometer data have been examined. Figure 7 is a plot of the results for 10-meV particles. One notes that these 10-meV particles scatter about the line of slope 0.5. The points tend to fall below the line at high absorption values and above the line at low absorption values. When the  $E \geq 20$  meV flux is plotted as the abscissa, the points at low absorption tend to fall below the line while those at high values tend to fall above the line. Thus, the square root of the absorption is directly proportional to the integral flux somewhere between 10 and 20 meV. Within the limitations of this analysis, therefore, the integral flux for  $E \geq 11$  meV is an experimentally verified conclusion. The constant of proportionality,  $K$ , from this curve is

$$K = 8 \pm 2$$

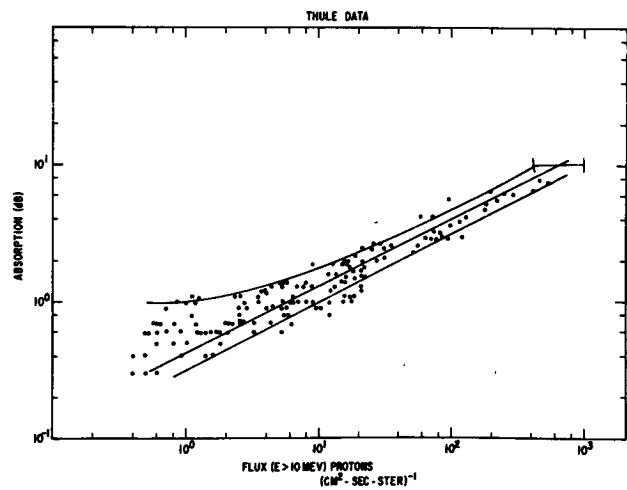


Figure 7. Riometer absorption at Thule as a function of the interplanetary proton flux ( $E \geq 10$  meV protons/cm<sup>2</sup>-sec-ster). If the square of the riometer absorption were proportional to the flux, the points would fall on the straight line.

## VI. Summary

An interdisciplinary approach to proton event prediction allows some effects to be calculated from first principles shortly after the optical flare occurs. Solar X-ray burst characteristics are useful in determining if protons were produced in sufficient quantity to give riometer absorption. The position of the flare on the solar disk and the solar wind velocity can be used to indicate the rise-time and peak intensity of the event in near earth space. Using the first few proton data points, the proton intensities

can be extrapolated into the future using previously derived values for the proton diffusion coefficients given in figure 6. Satellite data can be used to update the predictions during the event by extrapolating the fluxes as a function of time. Experimental measurements have verified some of the assumptions and theoretical predictions for 30 MHz riometer absorption. Thus, the satellite measurements can be employed to specify and predict proton fluxes and radio absorption. The approach taken in this report can be continued to give better predictions once more data become available.

## REFERENCES

1. ESSA Research Laboratories: "Solar Geophysical Data," *IER-FB-281 to IER-FB-295, 1967-1968.*
2. Carrigan, A. L.; and Oliver, N. J.: *Geophysics and Space Data Bulletin, IV-VI*, Air Force Cambridge Research Laboratories, 1967-1968.
3. Kuck, George A.: "Proton Events in 1967-1968," *Ionospheric Forecasting, AGARD Conference Proceedings No. 49*, Vaughn Agy, Editor, Paper #9, January 1970.
4. Singer, S.: "The Vela Satellite Program for Detection of High-Altitude Nuclear Detonations," *Proc. IEE, 53, 1935*, 1965. (Also, private communications.)
5. Conner, J. P.: Private communication, Los Alamos Scientific Laboratories.
6. Blocker, N.B.; Fehlau, et al., *Vela V and VI Solar X-Ray Atlas*, Los Alamos Scientific Laboratories Document LA-4454, Vols. I, II, and other volumes in preparation.
7. Zel'dovich, Ya. B.; Raizer, Yu. P.: *Physics of Shock Waves and High Temperature Hydrodynamic Phenomena*, Academic Press, N.Y., and London, 1966, Vol. 1.
8. Neupert, W. M.: "X Rays from the Sun," in *Annual Review of Astronomy and Astrophysics*, Vol 7, p. 121.
9. Burlaga, L. F.: "Anisotropic Diffusion of Solar Cosmic Rays," *J. Geophys. Res. Vol. 72, 4449*, 1967.
10. Parker, E. N.: *Interplanetary Dynamical Processes*, Interscience Publishers, New York, 1963.
11. Krimigis, S. M.: "Interplanetary Diffusion Model for the Time Behavior of Intensity in a Solar Cosmic Ray Event," *J. Geophys. Res., Vol. 70, 2943*, 1965.
12. Adams, G. W.; Masley, A. J.: "Theoretical Study of Cosmic Noise Absorption Due to Solar Cosmic Radiation," *Planet. Space Sci., Vol. 14, 1966*, p. 277.
13. Juday, R. W.; Adams, G. W.: "Riometer Measurements, Solar Proton Intensities, and Radiation Dose Rates," *Planet. and Space Sci., 17, 1313*, 1969.